Monte Carlo study of nanowire magnetic properties

R. Masrour[a)b)], L. Bahmad[a)†], and A. Benyoussef[b)]

[a)] *Laboratoire de Magnétisme et Physique des Hautes Energies, URAC* 12, *Université Mohammed V-Agdal, Faculté des Sciences, B.P.* 1014, *Rabat, Morocco*

[b)] *Laboratory of Materials, Process, Environment and Quality, Cady Ayyad University, National School of Applied Sciences, Safi, Morocco*

(Received 7 September 2012; revised manuscript received 3 December 2012)

In this work, we use Monte Carlo simulations to study the magnetic properties of a nanowire system based on a honeycomb lattice, in the absence as well as in the presence of both an external magnetic field and crystal field. The system is formed with N_L layers having spins that can take the values $\sigma = \pm 1/2$ and $S = \pm 1, 0$. The blocking temperature is deduced, for each spin configuration, depending on the crystal field Δ. The effect of the exchange interaction coupling J_p between the spin configurations σ and S is studied for different values of temperature at fixed crystal field. The established ground-state phase diagram, in the plane (J_p, Δ), shows that the only stable configurations are: $(1/2, 0), (1/2, +1)$, and $(1/2, -1)$. The thermal magnetization and susceptibility are investigated for the two spin configurations, in the absence as well as in the presence of a crystal field. Finally, we establish the hysteresis cycle for different temperature values, showing that there is almost no remaining magnetization in the absence of the external magnetic field, and that the studied system exhibits a super-paramagnetic behavior.

Keywords: Monte Carlo simulations, nanowire, magnetic field, crystal field

PACS: 75.75.+a, 77.80.B–, 71.70.Gm, 61.46.Fg **DOI:** 10.1088/1674-1056/22/5/057504

1. Introduction

During the last decade, one could observe a growing interest in the experimental and theoretical investigation on several nanostructures.[1–4] Nanowires are especially attractive for nanoscience studies as well as for nanotechnology applications. Since the discovery of compounds formed with carbon nanowires,[5] the magnetic properties of the nanometric-scale materials have been attracting considerable attention. Different geometric configurations are included in these structures, such as fullerenes and nanowires. The exploration of different properties of these objects opens a wide perspective for a great number of experimental applications. One of the potentially interesting aspects of these nano-physical systems is related to their magnetic properties. Experimental studies have been carried out to underline the magnetic properties of nanowires.[6,7] Nanowires, compared with other low-dimensional systems, have two quantum confined directions, while still leaving one unconfined direction for electrical conduction. This allows nanowires to be used in applications where electrical conduction, rather than tunneling transport, is required. Because of their potential application in high-density magnetic recording media, magnetic nanowire and nanowire arrays have received growing interest. Among them, transition metal alloys include CoPt, CoPd, FePt, and FePd alloys.[8–12] The effect of an external magnetic field applied during electro-deposition on magnetic properties of CoPt nanowires has been studied.[13] Furthermore, nanowires have been shown to provide a promising framework for the design of nanostructures, nanoscience investigation, and potential nanotechnology applications. On the other hand, the Monte Carlo simulations have been carried out to investigate the magnetic properties of nano-systems, including nano-graphene systems.[14–22]

In this work, we carry out Monte Carlo simulations to study nanowire magnetic properties, based on a honeycomb lattice and a finite number of layers. We deduced the thermal magnetization and susceptibility for two spin configurations σ and S. The blocking temperatures as well as the hysteresis cycle are obtained, in the absence as well as in the presence of both an external magnetic field and crystal field.

2. Theoretical model

The Hamiltonian governing the studied system is given by

$$H = J_1 \sum_{\langle i,j \rangle} \sigma_i \sigma_j - J_2 \sum_{\langle i,j \rangle} S_i S_j - J_p \sum_{\langle i,j \rangle} \sigma_i S_j + h \sum_i (\sigma_i + S_i) + \Delta \sum_j S_j^2, \quad (1)$$

where $\langle i, j \rangle$ stands for the nearest neighbors between the spins $\sigma_i = \pm 1/2$ and spins $S_j = \pm 1, 0$ (see Fig. 1); J_1 stands for the coupling constant between the spins (σ_i, σ_j), and J_2 is the coupling constant between the spins (S_i, S_j); J_p denotes the coupling constant between the spins σ_i and S_j; the crystal field Δ is applied only on the spins S, whereas the external magnetic field h acts on all the spins σ_i and S_j. A sketch of the geometry of the studied nanowire system is illustrated in Fig. 1. In this

†Corresponding author. E-mail: bahmad@fsr.ac.ma

© 2013 Chinese Physical Society and IOP Publishing Ltd

work, the coupling constants are fixed at $J_1 = J_2$=1 K. Unless otherwise stated, we set $J_p = -1$ K.

Starting from the above Hamiltonian (Eq. 1), one can investigate the total energy of the system as follows:

$$E_T = E_\sigma + E_S + E_P + E_{h\sigma} + E_{hS} + E_d, \tag{2}$$

where the exchange energy between spins σ is

$$E_\sigma = -J_1 \sum_{k=1}^{N_L} \sum_{j=1}^{N_\sigma} \sigma_j^k \left(\sigma_{j-1}^k + \sigma_{j+1}^k + \sigma_j^{k-1} + \sigma_j^{k+1} \right), \tag{3}$$

the exchange energy between spins S is

$$E_S = -J_2 \sum_{k=1}^{N_L} \sum_{j=1}^{N_S} S_j^k \left(S_{j-1}^k + S_{j+1}^k + S_j^{k-1} + S_j^{k+1} \right), \tag{4}$$

and the exchange energy between spins σ and S is

$$E_p = -J_p \sum_{k=1}^{N_L} \sum_{j=1}^{N_\sigma} \sigma_j^k \left(S_{2j}^k + S_{2j-1}^k + S_{2j-2}^{k+1} \right). \tag{5}$$

The Zeeman energies for the spins σ and S are

$$E_{h\sigma} = h \sum_{k=1}^{N_L} \sum_{j=1}^{N_\sigma} \sigma_j^k, \quad E_{hS} = h \sum_{k=1}^{N_L} \sum_{j=1}^{N_S} S_j^k. \tag{6}$$

Finally, since the crystal field acts only on the spins S, the corresponding energies are expressed as

$$E_d = \Delta \sum_{k=1}^{N_L} \sum_{j=1}^{N_S} (S_j^k)^2. \tag{7}$$

We use free boundary conditions for the extreme layers: $k = 0$ and $k = N_{L+1}$, so that

$$\begin{cases} \sigma_j^0 = \sigma_j^{N_L+1} = 0, & (j = 1,2,\ldots,N_\sigma), \\ S_j^0 = S_j^{N_L+1} = 0, & (j = 1,2,\ldots,N_S). \end{cases} \tag{8}$$

For a fixed layer k $(1 \le k \le N_L)$, we impose the cyclic conditions on the spins σ as well as for the spins S

$$\begin{cases} \sigma_0^k = \sigma_{N_\sigma}^k, & (k = 1,2,\ldots,N_L), \\ S_0^k = S_{N_S}^k, & (k = 1,2,\ldots,N_L). \end{cases} \tag{9}$$

It is worth noting that the studied model and the established equations are valid for any values of the parameters N_L, N_σ, and N_S. However, in this work, we will present numerical results for fixed values of these parameters: $N_L = 6$, $N_\sigma = 12$, and $N_S = 7$.

3. Monte Carlo simulations

The nanowire geometry of the studied system is illustrated in Fig. 1, where both the spins σ and spins S are located on a honeycomb lattice, with 6 layers in total. We performed the Monte Carlo simulations with Metropolis algorithm for standard sampling method to simulate the Hamiltonian given by Eq. (1). Free boundary conditions on the nanowire lattice are imposed only for the layers N_L+1 and N_0, and cyclic conditions are used for a fixed layer: $1 \le k \le N_L$. Starting from an initial spin configuration, other sequential configurations are generated when making single-spin flip attempts. The flips are accepted or rejected according to a heat-bath algorithm, using the energies given by Eqs. (2)–(7).

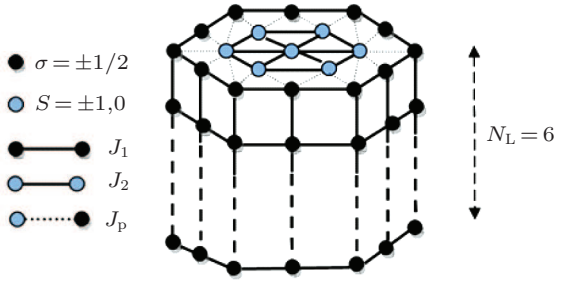


Fig. 1. (color online) A sketch of the geometry of the studied system formed with a nanowire with spins $\sigma = \pm 1/2$ (dark circles), and $S = \pm 1, 0$ (gray circles). Here, $N_\sigma = 12$, $N_S = 7$, and $N_L = 6$ for two spin configurations.

Starting from different initial conditions, we average each parameter over many configurations by the Monte Carlo simulations using the Metropolis algorithm. We perform 10^5 Monte Carlo steps (MCS) for each spin configuration, with the first 10^4 generated configurations discarded.

The formulas of the parameters of interest are given below. The internal energy per site is

$$E = \frac{1}{N_L(N_s + N_S)} \langle E_T \rangle . \tag{10}$$

The magnetizations per site are

$$M_\sigma = \left\langle \frac{1}{N_L N_\sigma} \sum_{k=1}^{N_L} \sum_{j=1}^{N_\sigma} \sigma_j^k \right\rangle, \tag{11}$$

$$M_S = \left\langle \frac{1}{N_L N_S} \sum_{k=1}^{N_L} \sum_{j=1}^{N_S} S_j^k \right\rangle. \tag{12}$$

The total magnetization is $M_{tot} = (M_\sigma + M_S)/2$. The magnetic susceptibilities are given by

$$\chi_\sigma = \beta \left(\langle M_\sigma^2 \rangle - \langle M_\sigma \rangle^2 \right), \tag{13}$$

$$\chi_S = \beta \left(\langle M_S^2 \rangle - \langle M_S \rangle^2 \right), \tag{14}$$

where $\chi_{tot} = (\chi_S + \chi_\sigma)/2$ is the total susceptibility, $\beta = 1/k_B T$, k_B is the Boltzmann constant ($k_B = 1$), and T denotes the temperature.

4. Results and discussion

The ground-state phase diagram in plane (J_p, Δ) of nanowire structure is illustrated in Fig. 2. The only stable phases are $(1/2,0)$, $(1/2,1)$, and $(1/2,-1)$.

The phase $(1/2,-1)$ is the only stable phase in the region of $J_p \leq 0$ and $\Delta \leq -6J_p/13+55/13$. While for $J_p \geq 0$ and $\Delta \leq +6J_p/13+55/13$, the only stable phase is found to be the phase $(1/2,+1)$ in this region of the plane (J_p, Δ). The phase $(1/2,0)$ is stable for all J_p values, provided that the crystal field satisfies

$$\begin{cases} \Delta \geq -\left(\dfrac{6}{13}\right)J_p + \dfrac{55}{13}, & (J_p < 0), \\ \Delta \geq +\left(\dfrac{6}{13}\right)J_p + \dfrac{55}{13}, & (J_p > 0). \end{cases}$$

In the particular case $J_p = 0$, the three phases exist, depending on the crystal field values. This case is not interesting, since the spins σ and S are disconnected, and the crystal field only acts on the spins S.

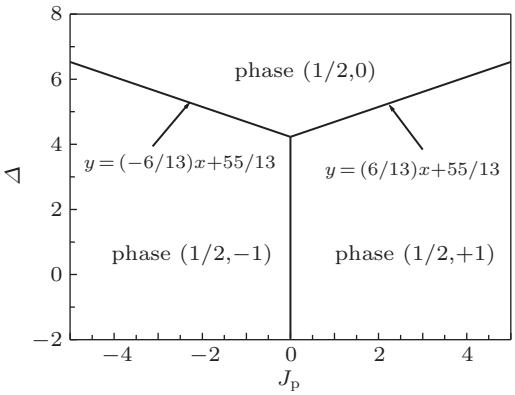


Fig. 2. Ground state phase diagram in the (J_p; Δ) plane for the studied nanowire formed with two spin configurations: σ and S. The only stable configurations are $(1/2,0)$, $(+1/2,+1)$ and $(1/2,-1)$.

Figures 3(a) and 3(b) illustrate the thermal variation of the magnetization M_σ and magnetic susceptibility χ_σ for the spins σ, in the absence ($\Delta = 0$) and presence of a crystal field ($\Delta = 3$), respectively. It is found that the crystal field has the effect of decreasing the blocking temperature $T_B(\sigma)$ from 4.2 K ($\Delta = 0$) to 2.2 K ($\Delta = 3$) for the spins σ.

In order to show the crystal field effect on the spins S, we plot the thermal variation of magnetization M_S and magnetic susceptibility χ_S for the spin S in the absence ($\Delta = 0$) and presence of magnetic crystal field ($\Delta = 3$) in Figs. 4(a) and 4(b), respectively. Once again, the obtained blocking temperature $T_B(S)$ for the spins S, decreases in the presence of a magnetic crystal field. In fact, the blocking temperature $T_B(S)$ decreases from 4.7 K when $\Delta = 0$ to 2.6 K when $\Delta = 3$. It is worth noting that these values are comparable with those obtained in other literature when using Monte Carlo investigation for Ising nanowires and nanostrips (for example, see Ref. [23]).

For very low temperatures, the saturation magnetizations of the nanowires for the spins σ and S are 0.5 and 1 emu·g^{-1}, respectively. This is in good agreement with the ground-state phase diagram shown in Fig. 2.

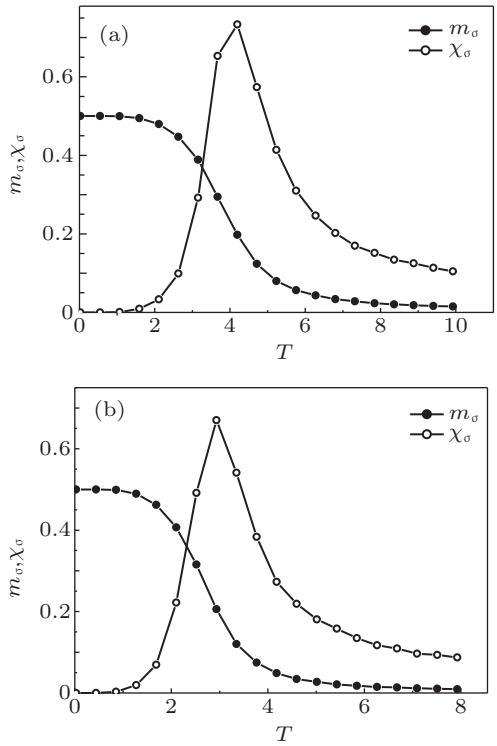


Fig. 3. Magnetization M_σ and magnetic susceptibility χ_σ versus the temperature for the spin configuration σ (a) in the absence of the crystal field ($\Delta = 0$) and (b) in the presence of the crystal field ($\Delta = 3$).

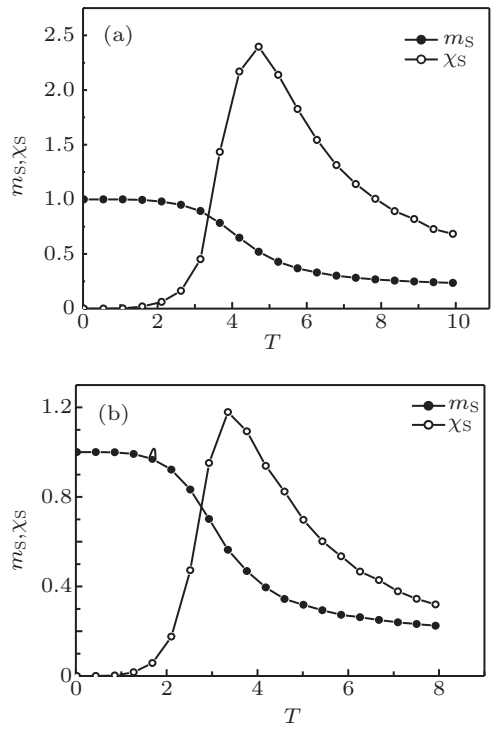


Fig. 4. Magnetization M_S and magnetic susceptibility χ_S versus the temperature for the spin configuration S (a) in the absence of the crystal field ($\Delta = 0$) and (b) in the presence of the crystal field ($\Delta = 3$).

In Fig. 5, we present the total magnetization versus the exchange interaction J_p for different values of crystal field ($\Delta = 0.0, 2.0, 2.5$) at a fixed temperature $T = 3$ K. For negative values of the coupling constant J_p, it is found that the total nanowire magnetization remains nearly constant ($M_{tot} \approx 0.25$ emu·g^{-1}). The total nanowire magnetization is not affected by increasing crystal field from 0.0 to 2.5. However, for positive exchange interaction J_p between the spins σ and S, figure 5 shows that the total nanowire magnetization strongly depends on the applied crystal field. These magnetizations vanish with increasing crystal field.

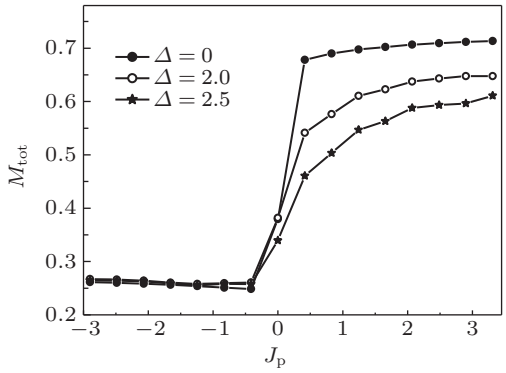


Fig. 5. Total magnetization M_{tot} versus the exchange interaction J_p for $\Delta = 0.0, 2.0, 2.5$, at a fixed temperature $T = 3$ K.

As shown in Figs. 3(b) and 4(b), the blocking temperature for the spin-S configuration, is higher than that one of the spin-σ configuration, for a fixed magnetic crystal field. In fact, this finding is valid for an arbitrary value of the crystal field in the absence of the external magnetic field ($h = 0$), as shown in Fig. 6.

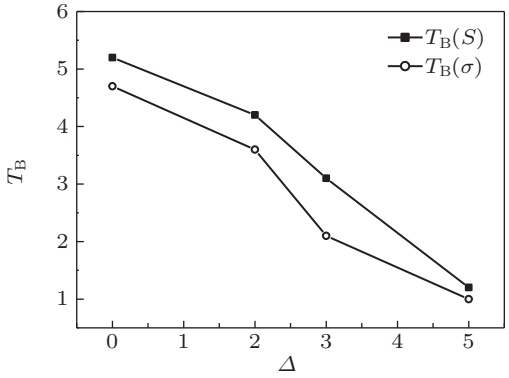


Fig. 6. Blocking temperature T_B versus the crystal field for the two spin configurations σ and S, in the absence of the external magnetic field ($h = 0$).

To complete this study, we will now investigate the effect of an external magnetic field, on the studied nanowire system. For this purpose, we present the total magnetization (M_{tot}) versus the external magnetic field h in the absence of the crystal field ($\Delta = 0$) and two fixed temperature values: 1.5 K and 2.5 K. It is found that the remanent magnetic field H_r and the total saturation magnetization of the nanowire are 0.58 Oe and 0.25 emu·g^{-1}, respectively. This indicates that there was almost no remaining magnetization in the absence of an external magnetic field, suggesting that the nanowire exhibits a superparamagnetic behavior.

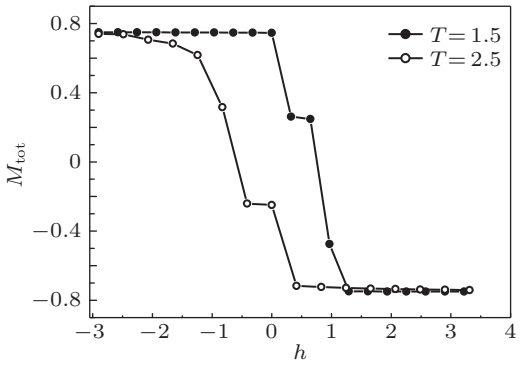


Fig. 7. Total magnetization M_{tot} as a function of the external magnetic field h for $T = 1.5$ and 2.5 K in the absence of the crystal field ($\Delta = 0$).

5. Conclusion

The magnetic properties of the Ising model on a nanowire lattice with 12 spin-σ ($\sigma = \pm 1/2$) configurations and 7 spin-S ($S = \pm 1, 0$) configurations for $N_L = 6$, are studied by Monte Carlo simulations.

In two configurations of spins, the magnetization decreases almost to zero with increasing temperature. The magnetic susceptibility reaches the maximum at the blocking temperature. The total magnetization increases with increasing exchange interaction J_p and decreases when increasing the crystal field at a fixed temperature. The blocking temperature decreases with increasing crystal field for $h = 0$.

The magnetization versus the magnetic field h for bilayers with spins σ and S versus external field shows magnetic hysteresis loops. The magnetic remanence M_r of the sample was 0.5 emu/g. This indicates that there is almost no remaining magnetization when the external magnetic field is removed, suggesting that nanowires exhibit a superparamagnetic behavior. The saturation magnetization and magnetic remanence are obtained for spin-σ and spin-S configurations.

References

[1] Harris P J F 1991 *Carbon Nano-wires and Related Structures: New Materials for the Twenty-first Century* (Cambridge: Cambridge University Press)
[2] Ball P 1993 *Designing the Molecular World: Chemistry at the Frontier* (Princeton, NJ: Princeton University Press)
[3] Dresselhaus M S, Dresselhaus G and Eklund P C 1996 *Fullerens and Carbon Nano-wires* (San Diego: Academic Press)
[4] *Carbon Nano-wires: Preparation and Properties* 1997 (ed. by Ebbesen T W) (Boca Raton, FL: CRC Press)
[5] Iijima S 1991 *Nature* **56** 354

[6] Escrig J, Landeros P, Altbir D, Vogel E E and Vargas P 2007 *J. Magn. Magn. Mater.* **308** 233
[7] Lü B, Xu Y, Wu D and Sun Y 2008 *Particuology* **6** 334
[8] Gao J H, Zhan Q F, He W, Sun D L and Cheng Z H 2005 *Appl. Phys. Lett.* **86** 232506
[9] Peng Y, Cullis T, Mobus G, Xu X J and Inkson B 2007 *Nanotechnology* **18** 485704
[10] Hu H N, Chen H Y and Yu S Y 2006 *J. Magn. Magn. Mater.* **299** 170
[11] Schaaf P, Zhang K, Lange C, Holz A, Weisheit M and Fähler S 2007 *Appl. Surf. Sci.* **253** 8107
[12] Takata K M and Sumodjo P T A 2007 *Electrochimica Acta* **52** 6089
[13] Liu H R, Lu Q F, Han X F, Liu X G, Xu B S and Jia H S 2012 *Appl. Surf. Sci.* **258** 7401
[14] Konstantinova E 2008 *J. Magn. Magn. Mater.* **320** 2721
[15] Bahmad L, Masrour R and Benyoussef A 2012 *J. Supercond. Nov. Magn.* **25** 2015
[16] Masrour R, Bahmad L and Benyoussef A 2012 *J. Magn. Magn. Mater.* **324** 3991
[17] Bahmad L, Benyoussef A and Ez-Zahraouy H 2002 *Phys. Rev. E* **66** 056117
[18] Xiao C M and Li C S 2007 *Acta Phys. Sin.* **56** 2434 (in Chinese)
[19] Xiao S, Liu M Z, Shang J and Wang H 2012 *Chin. Phys. B* **21** 020514
[20] Xiao S, Liu M Z, Wang J J and Wang H 2011 *Chin. Phys. B* **20** 060509
[21] Zhu Z L, Ding Y L, Wang Z Y, Gu J H and Lu J X 2010 *Chin. Phys. B* **19** 106803
[22] Xiao S, Cai J J, Wang R L, Liu M Z and Liu F 2009 *Chin. Phys. B* **18** 5103
[23] Garcia C, Martinez M F and Gonzalo J A 2003 *Phys. Rev. B* **68** 024510